



An 'isolated diffusion' gravimetric calibration procedure for radar and microwave moisture measurement in porous building stone

Scott Allan Orr ^{a,*}, Maureen Young ^b, Dawson Stelfox ^c, Alick Leslie ^d, Joanne Curran ^c, Heather Viles ^a

^a School of Geography and the Environment, University of Oxford, South Parks Road, Oxford OX1 3QY, United Kingdom

^b Historic Environment Scotland, The Engine Shed, Stirling, Forthside Way, Stirling FK8 1QZ, United Kingdom

^c Consarc Design Group, The Gas Office, 4 Cromac Quay, Ormeau Road, Belfast BT7 2JD, United Kingdom

^d Formerly Historic Environment, Scotland, United Kingdom

ARTICLE INFO

Article history:

Received 9 August 2018

Received in revised form 30 January 2019

Accepted 1 February 2019

Available online 6 February 2019

Keywords:

Natural stone

Cultural heritage

Infrastructure

Modelling

Material properties

GPR

ABSTRACT

Information about the presence and movement of water is crucial to understanding stone deterioration and rock weathering but hard to obtain. Non-destructive, non-invasive measurements of electromagnetic phenomena can provide proxy data on water contents within porous stone and rock. Commercial geophysical devices, such as radar and microwave moisture sensors, produce raw data or readings in arbitrary units, but can be related to absolute water contents through gravimetric calibration. Calibration procedures typically either equilibrate samples to a set of relative humidities (RH%) using salt solutions or environmental chambers (requiring specialised equipment), or monitor ambient drying which yields less homogenous moisture distributions and takes time. This study proposes and tests a cost- and time-effective 'isolated diffusion' gravimetric calibration procedure in which a set of samples are sealed at specific water contents and equilibrated. The procedure is compared to ambient drying over 120 h for three United Kingdom building stones and evaluated with modelled reflection coefficients and relative permittivities. The calibrations determined from isolated diffusion more closely follow modelled behaviour than those from ambient drying, as the calibrations developed from the latter were affected by uneven distributions of moisture. Calibrations for radar measurements developed from two types of back interfaces (air and metal) were very similar to one another, suggesting that measurements are consistent regardless of the type of back interface used. The isolated diffusion calibration procedure provides a cost-effective and simple method to facilitate comparison between different non-destructive testing methods and enables accurate measurement of water contents in porous geomaterials.

© 2019 The Authors. Published by Elsevier B.V. This is an open access article under the CC BY license (<http://creativecommons.org/licenses/by/4.0/>).

1. Introduction

Stone is weathered by a range of physical, biological, and chemical processes – most of which are propagated or caused by the presence and movement of moisture. How water will contribute to or cause different deterioration mechanisms depends on its spatial and temporal patterning (Mamillan, 1981). Stone is very commonly employed in historic buildings and traditional constructions; in the built context, water can be introduced into a building fabric in several ways. Understanding these ingress pathways is fundamental to management and conservation of the historic built environment.

Determining where moisture is and in what quantity is difficult because there are few techniques that directly measure it. The most straightforward is gravimetry, i.e. measuring the mass of water. Using this method in situ requires invasive sampling (typically core drilling) resulting in irreversible changes to the fabric of a building. Invasive

sampling or destructive testing constitutes a change in the historic building fabric and have limited spatial and temporal coverage. Even if undertaken for diagnostic purposes, this is restricted by administrative and ethical limitations.

Alternatively, indirect (non-destructive) testing methods can be used. Non-destructive testing (NDT) uses physical properties as proxies for moisture, such as electrical, visual, or thermal measurements. Many technologies have been developed or adapted for this purpose and have been thoroughly reviewed elsewhere (Pinchin, 2008; Camuffo and Bertolin, 2012; Saïd, 2007). Geophysical techniques such as radar and microwave are useful as the influence of salinity is negligible on the measurements within most of the microwave frequency range (Klein and Swift, 1977).

The output from a non-destructive measurement can be a physical property (such as electrical resistivity) or some transformation related to it. This transformation can be beneficial when a device is primarily designed for use on a particular type of material, or if the range of the property between dry and saturated states overlaps with potential water contents. In the latter case, the arbitrary scale reduces the risk

* Corresponding author.

E-mail address: scott.orr@ouce.ox.ac.uk (S.A. Orr).

of mistaking the physical property measured for an inferred water content.

To better understand and compare these indirect measurements, they can be calibrated to gravimetric measurements of laboratory samples. This creates a relationship between the physical property (or arbitrary scale) and the water content on a mass or volume basis. Calibrations can also be compared to models. Many standards are concerned with measuring moisture contents of traditional building materials (BSI, 2017. BS EN 16682, 2017; ISO, 2003; ASTM International, 2016). However, these are designed to quantify water contents in obtained samples through gravimetry, and do not contain procedures for calibrating non-destructive techniques.

Gravimetric calibrations of non-destructive moisture measurement devices use the mass of water as an accepted standard of the absolute measurement of the quantity of water present in a sample. This is important for cases in which moisture thresholds are of interest. In other scenarios, it might be more important to characterise general behaviours or ‘curve shapes’, as demonstrated elsewhere (Eklund et al., 2013). A subset of these are conceptually represented in Fig. 1. These allow an operator to understand how the device readings relate to water contents more broadly for a given material, without necessarily converting to quantitative water content. Fig. 1 demonstrates several conceptual shapes for calibration curves that might develop for commercial geophysical devices. In Fig. 1, the scenario presented in (a) the device is equally sensitive to the entire range of water contents of interest; (b) represents the scenario in which there is a different levels of sensitivity to changes in water content across the range of interest; (c) illustrates the potential challenge of measurement thresholds; the nature of the relationship is uncertain, as it might be closer to those in (a) or (b), or a combination thereof; (d) demonstrates a case of an inconsistent relationship with water contents. These inconsistencies can arise from several factors, including operator error, limitations of the technique and/or device, and material properties. These relationships are important to characterise to accurately interpret device output in the context of moisture contents.

Standards that do contain procedures for gravimetric calibration (ASTM International, 2013b, ASTM International, 2013a) are for wooden materials and primarily intended for use with electrical resistance and capacitive techniques. The current state-of-the-art recommends calibration be done by producing a range of relative humidity

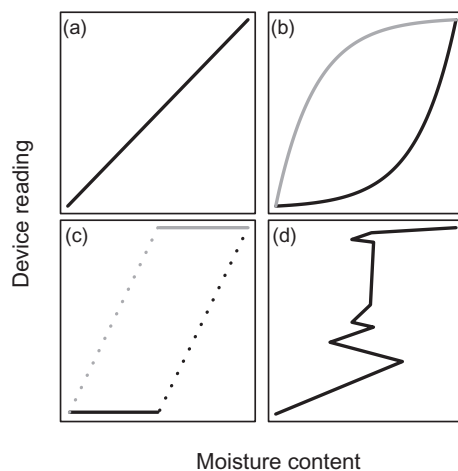


Fig. 1. Conceptual shapes of calibration curves for commercial geophysical devices. (a) represents the ideal calibration curve, with a consistent linear relationship; (b) shows non-linear relationships in which there is greater sensitivity at higher water contents (black) and lower water contents (grey); (c) a device that has thresholds of detection within the water content range of interest (black: lower, grey: upper); the nature of the relationship is uncertain, as it might be closer to those in (a) or (b), or a combination thereof; (d) a generally related trend in device readings that is inconsistently related to water content.

conditions using salt solutions and climatic chambers (Climent et al., 2018). These techniques require specialised facilities and equipment that can be costly to implement and operate, while also requiring significant amounts of time to develop calibrations.

Many factors can influence gravimetric calibration results, including material properties, sample size, environmental conditions, frequency of measurement, and the range of water contents. An uneven distribution of moisture within a sample might result in a false relationship with the gravimetry, since gravimetry calculations assume a homogeneous distribution. This is of particular concern for calibrations produced from ambient drying.

The benefits of employing multiple NDT techniques are widely acknowledged. Studies in the past have shown that applying multiple techniques will often provide the most information, yielding the best assessments (Martínez-Garrido et al., 2018; Martinho et al., 2014; Di Tullio et al., 2010; Válek et al., 2010). Combining radar and microwave measurement systems characterises variation in moisture in two spatial scales. Unfortunately, this is complicated not only by the difficulty of interpreting results from a single method but also the harmonisation of the results (Binda et al., 2010). Robust gravimetric calibration techniques can enable comparison by translating device output into absolute water contents as a common parameter. Thus, the choice of calibration procedure influences the precision and accuracy of multi-method surveys.

The MOIST350B microwave moisture system (hf sensor; Leipzig, DE) has been evaluated in laboratory and in situ with varying results. Bläuer and Rousset decried strongly that the microwave system had “too big [sic] flaws to be used in ... cultural heritage conservation” (Bläuer and Rousset, 2009, p. 32). They investigated how the microwave system monitored water vapour and liquid water uptake in Swiss building stones with little success (Rousset and Bläuer, 2009). Their testing scenario is limited in two ways: 1) water in the vapour phase introduces small changes in the dielectric properties of air (Birnbaum and Chatterjee, 1952), and 2) monitoring capillary rise (which is characterised by strongly heterogeneous distributions of water in a sample) introduces complex interactions with the aforementioned exponential loss pattern. Evaluations of brick have been more successful: the microwave system has shown good agreement with nuclear moisture density gauge readings but were noisier (Møller and Olsen, 2011). Gärtner et al. produced very strong gravimetric calibrations from historic brick samples extracted from a German concert hall that were then applied to other parts of the same building (Gärtner et al., 2010). However, we caution against the presentation of the calibrated sensor values they have employed: they have used the calibrations from four sensor heads to plot water contents at the maximum depths of penetration of each sensor. In reality, the moisture profile would be best represented by regression models of the four overlapping measurements, since they do not measure *at* a depth, but *to* a depth. More recently, unitless moisture indices measured on saturated and dry dolostone samples in layered configurations have agreed well with modelled microwave reflection coefficients (Kurik et al., 2017). In this research, the intermediate values (between dry and saturated states) were not examined. These studies do not use appropriate data collection and evaluation methods to determine this device's accuracy and utility in assessing a range of liquid moisture contents in natural building stones.

1.1. Objective

This study proposes a procedure for gravimetric calibration and demonstrates its implementation for radar and microwave measurements on three UK building stones. It is an innovative but straightforward method which to our knowledge has not yet been published using a vapour impermeable barrier to ‘isolate’ samples at a single water content – allowing equilibrium moisture diffusion throughout the sample. These calibrations are evaluated with models of effective

dielectric permittivity and electromagnetic reflection and transmission coefficients to determine their applicability for evaluating and comparing radar and microwave moisture measurement.

2. Material and methods

2.1. Stones

This study investigated gravimetric calibrations for three stone types (Table 1): Portland limestone (base bed), Locharbriggs sandstone, and Clipsham limestone. These are common building and repair stones in the UK, which are susceptible to a range of weathering mechanisms. The samples were cubic (150 mm × 150 mm × 150 mm), as determined by the field of detection of the deepest microwave moisture sensor.

2.1.1. Portland

Commonly found throughout the world as a building and repair stone. In the UK, it has been used for prominent buildings such as St Paul's Cathedral, London (Inkpen et al., 2012). It is now quarried in the Isle of Portland off the south coast of England. It is an Upper Jurassic limestone that is dominated by small to medium grain sizes (Leary, 1983; Jaynes and Cooke, 1987), with a matrix-rich compacted texture (Dubelaar et al., 2003). The base bed is homogenous with very few oolites or visible bedding planes.

2.1.2. Locharbriggs

A Permian sandstone from Dumfries, Scotland that has been quarried since the 18th century. It is a pink to red medium grained sandstone (Building Research Establishment, 2000) widely used across Scotland and England for traditional masonry styles and contemporary cladding. It is characterised by distinctive aeolian cross lamination and is composed mainly of quartz, with some feldspars and clays and very few small rock fragments (Pandey et al., 2014).

2.1.3. Clipsham

A Middle Jurassic, very pale cream and buff oolitic limestone from Lincolnshire, England. It is coarse-grained and contains many small patches of a light brown colour (Emery and Dickson, 1989). The oolites are of a variety of shapes and sizes and there are also shell fragments and very small pebbles. It was probably deposited in a moderately sub-tropical sea, where changes were frequent, making its texture liable to a certain amount of variation. Clipsham has been used extensively as a repair stone for other oolitic limestones in the south of England, but also as a historical building stone such as a 15th century tower at Eton College (Braun and Wilson, 1970).

2.2. Procedure

Two contrasting methods for gravimetric calibrations have been compared for radar and microwave techniques. The first procedure uses a stone sample dried over time in ambient conditions, while the second uses vapour impermeable materials to 'isolate' samples at a

single water content – encouraging equilibrium moisture diffusion throughout the sample. These calibrations are evaluated with models of electromagnetic reflection and transmission coefficients and effective dielectric permittivity.

2.3. Equipment

2.3.1. Radar

Originally applied in near-surface geophysical investigations, radar has become a powerful imaging and diagnostic technique in civil engineering for building applications (Lai et al., 2017). This study has used a 1.6 GHz GPR antenna (Malå Geoscience, Malå, Sweden).

To identify water contents, amplitudes and travel times of features can be extracted from individual A-scans (Fig. 2). The amplitude of the direct wave is contributed to by the surface reflection, i.e. the difference between the relative permittivity between the materials on either side of the surface interface ($\epsilon_{r, air}$ and the bulk material $\epsilon_{r, b}$). The higher the water content, the greater the difference between $\epsilon_{r, air}$ and $\epsilon_{r, b}$. This results in a reduced reflection amplitude, i.e. higher transmission.

An electromagnetic signal will travel with a reduced velocity in a sample with higher water contents. This can be represented by the signal travel time between the direct wave t_d (the reflection from the surface) and the reflected wave t_r (the reflection generated by the interface at the back of the sample), also referred to as the reflector (Galagedara et al., 2003) or 'back-wall reflection' (Lai et al., 2014). This method of assessing water contents with radar has been called the 'depth to a known reflector' method (Elkarmoty et al., 2018), is well-represented in literature (ASTM International, 2011. D6432-11, 2011; Cetrangolo et al., 2017), and is well illustrated by Lai et al. (2014); see their (Fig. 5). The travel time of the surface wave t_s must also be accounted for in the calculation, which is equal to the ratio of the distance between the source and the receiver d_{sr} (60 mm for the Malå 1.6 GHz antenna; Pérez-Gracia et al. (2009)) and the speed of light c . The corrected travel time t_c is represented by $t_c = t_r - t_d - t_s$.

The travel time can be converted into an average velocity $\bar{v} = 2z/t_c$ from the corrected travel time t_c and wall thickness z . Capitalising on $\bar{v} \approx c \times (\epsilon_r)^{-1/2}$, the real component of relative permittivity (often referred to as the dielectric constant) can be expressed as:

$$\epsilon'_r = \left(\frac{ct_c}{2z} \right)^2 \quad (1)$$

Both the amplitude and travel time method can be represented in a number of ways and are influenced by certain procedural details. The reflective wave can often be quite weak. However, because a metal plate has infinite values of dielectric, it can reverse the signal amplitude polarity (Senin and Hamid, 2016), resulting in a transformed A-scan represented by the grey line in Fig. 2. If this occurs, selecting the 'primary' peak of the wave can be ambiguous; in Fig. 2, this could be represented by either the upper a_u or lower a_l amplitudes. It is advantageous to measure the wave amplitude with the peak-to-peak summed

Table 1

Hygic and physical properties of the three stone types investigated in this study.

| Procedure | Number of samples | Density/kg m ⁻³ | Water content _{sat} ^a /% | Effective porosity ^b /% |
|------------------------|-------------------|----------------------------|--|------------------------------------|
| Ambient drying | | | | |
| Portland limestone | 1 | 2378 | 4.9 | 11.7 |
| Clipsham limestone | 1 | 2371 | 4.7 | 11.2 |
| Locharbriggs sandstone | 1 | 1991 | 8.5 | 17.0 |
| Isolated diffusion | | | | |
| Portland limestone | 6 | 2244–2291 | 5.1–5.2 | 11.5–11.8 |
| Clipsham limestone | 6 | 2363–2391 | 4.0–4.7 | 9.57–11.2 |
| Locharbriggs sandstone | 6 | 2033–2161 | 6.5–8.5 | 14.0–17.4 |

^a by mass, dry basis, water content_{sat} = $m_{\text{water}}/m_{\text{bulk}} \times 100\%$

^b equivalent to saturated water content, effective porosity $f = v_{\text{water}}/v_{\text{bulk}} \times 100\%$

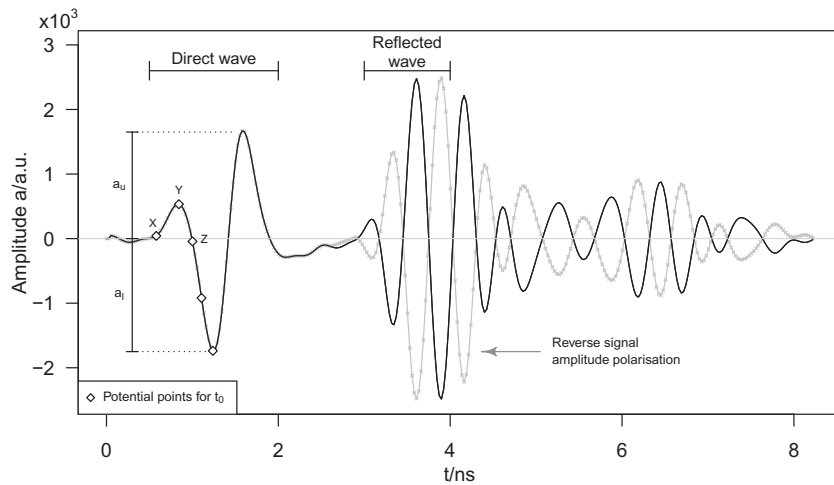


Fig. 2. A demonstrative A-scan taken on an oven-dry sample of Portland limestone 150 mm×150 mm×150 mm. The potential points for t_0 within the direct wave were identified with a practitioner and expert survey (Yelf, 2004).

amplitude, i.e. with $a_p = a_u + a_l$ the absolute difference between the positive and negative peaks within the wave.

For calculating travel times, there is no consensus on where ‘time zero’ is within the direct wave (Yelf, 2004). Any number of parameters may be used, including (see Fig. 2 for letter references): the time where the signal starts to raise over a predefined threshold (X), the time of the first extreme value (Y), or the first zero crossing after the first extreme value (approximately Z) (RILEM TC 177-MDT, 2005; Rodríguez-Abad et al., 2016).

Radar has most frequently been used to identify water contents in concrete using both amplitude and travel time changes (Laurens et al., 2005; Klysz and Balayssac, 2007; Senin and Hamid, 2016), but has also been effectively employed for geological materials at low frequencies (Olatinsu et al., 2013) and brick specimens (Cetrangolo et al., 2017). Spectral analysis has been applied to A-scans (usually as a fast Fourier transform) to look at additional peak characteristics to the maxima and minima (Lai et al., 2014; Leucci et al., 2012).

2.3.2. Microwave moisture system

The MOIST350B (hf sensor; Leipzig, Germany) capitalises on the significant difference between the relative permittivity of water and most geological building materials in the microwave frequency region. The device works by producing an electromagnetic wave and measuring the proportion of energy that is reflected (the ‘reflection coefficient’) and measured by a receiving unit built into the sensor (Göller, 2006). A set of sensor heads penetrate to different depths by changing the field using combinations of certain antennae and applicators (Göller, 2001), but all operating within a narrow frequency range around 2.45 GHz, the Industrial, Scientific and Medical (ISM) radio band (International Telecommunication Union, 2016). Microwaves lose energy exponentially as they travel through materials like building stones (BSI, 2017). Therefore, all of the sensor heads (regardless of penetration depth), are sensitive to moisture near the surface. The three sensors used in this study have their respective penetration depth (Göller, 2012):

- R: up to 3 cm
- D: up to 10 cm
- P: up to 25 cm

Each sensor head includes a set of calibrations for typical building materials where the reflection coefficient is transformed into a percent water content. While these are named for broad categories of materials (e.g. ‘calcareous sandstone’), they were developed for one particular type of that material. In addition to these calibrations, a unitless

moisture index (MI) can be used, which is a set of arbitrary units related more directly to the reflection coefficient. Both material-specific calibrations and the MI values are picked from the set of reflection coefficients generated within a frequency band around 2.45 GHz in a variety of ways specified by the manufacturer.

2.3.3. General protocol

The two gravimetric calibration procedures (ambient drying vs isolated diffusion) differed in how the range of water contents was produced. Similar protocols were followed as part of each procedure. The tests were undertaken under laboratory conditions (18 to 22 °C and 40 to 60% RH). Mass measurements were taken with a balance capable of measuring up to 30 kg with a precision of ± 0.001 kg. The samples were oven-dried at 70 °C for 72 h and weighed to obtain the dry mass. Samples were then immersed in distilled water for 72 h and weighed to obtain the saturated¹ mass. For measurements taken immediately following the removal of samples from immersion, surface water was removed with an absorbent cloth.

In general, microwave fields are as wide as they are deep. To investigate the entire field of the P sensor, laboratory specimens would need to be at least 250 mm on each side, resulting in unwieldy samples weighing more than 30 kg each. Cubic samples of 150 mm in each dimension were selected as a compromise; it is presumed that the edge effects are negligible, since the dependence of microwave reflection decays exponentially with distance from the antenna.

Before each measurement, the mass of the sample was recorded to determine the water content. The radar measurements comprised of 81 A-scans for each face, and were recorded for both a back wall interface of air and a 3 mm metal plate. The microwave measurements were taken at the centre of each face, with the sample placed on a large block of granite to minimise interference from edge and back-reflection effects. Each value was based on an average of three measurements.

2.3.4. Ambient drying procedure

This method, used as a comparison for the proposed calibration procedure, is a variation of the calibration protocol formalised by Eklund et al. (Eklund et al., 2013). The samples of stone were removed from immersion and monitored during 120 h of drying in ambient laboratory conditions. Drying was uninhibited for five faces but partially covered

¹ In this study we define the saturation mass as a *pseudo-saturated*, or reduced saturation state, ignoring the effects of air trapping (Gummerson et al., 1980), see also (Hall and Hoff, 2012, p. 222)

for the sixth face as the samples were placed on a metal grid. Measurements were taken on each of the six faces every 24 h.

2.3.5. Isolated diffusion procedure

This new method uses multiple samples of a geomaterial that are each set to a particular water contents including and between oven-dry and saturated states. After being removed from immersion, the mass of the samples was periodically monitored. Once they reached the desired average water content, they were sealed in layers of polyethylene with vapour-resistant tape roughly 2 mm thick. The samples were left for 168 h to ensure that water diffused before measurements were taken. The samples were stored in sealed states but turned periodically (roughly every one to two weeks) to reduce gravitational effects.

One benefit of this procedure is that samples can be set to any range or subset water contents. In this study, five to six equally-spaced water contents ranging from oven-dry and saturated states were selected, depending on the stone type. If a sub-range of water contents was of particular interest, the procedure could be applied to these values instead of equally spaced water contents.

3. Theory/calculation

This section introduces the theory that underpins the interactions between electromagnetic energy and porous media. Calculations of modelled dielectric constants and reflection coefficients in porous media systems are presented, which represent expected behaviour of the radar and microwave techniques, respectively, over a range of water contents.

Radar and microwaves are forms of electromagnetic energy governed by the same underlying principles. Models of how they should interact with porous media systems produce a reference of how the techniques should theoretically respond to different water contents in building stones. These can be compared to the device measurements to assess the effectiveness of the techniques and calibration procedures.

Electromagnetic waves travel through media depending on three properties: the electrical conductivity σ , the dielectric permittivity ϵ , and the magnetic permeability μ . In building stones, μ is equal to the permeability in free space since they are non-magnetic. In the microwave frequency range, electromagnetic waves are influenced by both σ and ϵ and it is not possible to separate their effects. They are complex properties, the real and imaginary components denoted with prime ' and double prime " , respectively. A combined effective permittivity ϵ_e is derived from their summation (adapted from Laurens et al. (2005)):

$$\begin{aligned}\epsilon_e &= \epsilon + \frac{\sigma}{j\omega} \\ &= (\epsilon' - j\epsilon'') + \frac{\sigma' + j\sigma''}{j\omega} \\ &= \left(\epsilon' + \frac{\sigma'}{\omega}\right) - j\left(\epsilon'' + \frac{\sigma''}{\omega}\right) \\ &= \epsilon'_e - j\epsilon''_e\end{aligned}\quad (2)$$

where the conductivity is divided by the imaginary number j and the angular frequency ω . Generally, permittivities are expressed relative to the permittivity of air ϵ_0 as ϵ_r , i.e.

$$\epsilon_r = \frac{\epsilon_e}{\epsilon_0} = \frac{\epsilon'_e - j\epsilon''_e}{\epsilon_0} = \epsilon'_r - j\epsilon''_r\quad (3)$$

The real component ϵ'_r is the dielectric constant. The dielectric constant is related to the storage of energy in porous building materials (Sahin and Ay, 2004), while the imaginary component represents absorption losses and affects the signal attenuation.

The dielectric constant is a bulk property. Many models have been developed for representing multi-phase systems (Martinez et al., 2001; Knoll, 1996). Recently, microwave reflections from porous

building stones have been modelled (Kurik et al., 2017) with the two-phase mixed materials Maxwell Garnett formula (Maxwell Garnett, 1904; Sihvola, 2000). However, the system is comprised of three phases: the solid mineral content, the liquid water content, and the vapour water/air mixture. To reflect this, a Lichtenecker-Rother mixing model (Lichtenecker and Rother, 1931) has been used:

$$\epsilon_b^\alpha = \sum_i V_i \epsilon_i^\alpha\quad (4)$$

where α is a 'geometrical' or constant shape factor; when $\alpha = 0.5$, the mixing model describes refractive mixing (Dobson et al., 1985). Among a number of mixing models, this model (with $\alpha = 0.5$) was shown by Knoll (1996) to most closely match experimental data of Lundien (1966) and Newton (1977). When this model was applied for wet soil by Birchak et al. (Birchak et al., 1974) it included parameters for bound water: as this is negligible for the stones studied it has been omitted. We have defined a combined effective permittivity for the mineral-air combination $\epsilon'_{m,r}$. Since we are only representing wave velocity, only the real component ϵ'_b of the bulk relative effective permittivity (the bulk dielectric constant) has been presented as:

$$\epsilon'_{b,r} = \left[(1-f)\sqrt{\epsilon'_{m,r}} + f\sqrt{\epsilon'_{w,r}}\right]^2\quad (5)$$

in which f is the effective porosity, $\epsilon'_{w,r}$ is the dielectric constant of fresh water ($\epsilon'_{w,r} \approx 80$) and $\epsilon'_{m,r}$ is the dielectric constant of the combined solid-vapour phase material. At an oven-dry state $f \approx 0$, so Eq. (5) simplifies to $\epsilon'_{b,r} = \epsilon'_{m,r}$, which can be determined from an appropriately-treated laboratory sample via Eq. (1). Using the calculated value of $\epsilon'_{b,r}$ the dielectric constant can be modelled for a given sample as a function of water content.

The bulk (or adjusted) dielectric constant of a multi-layered system can be represented using a parallel plate capacitor model (Zhao, 2015). The calculated dielectric constant from isolated diffusion was adjusted to account for the 2 mm thick layer of polyethylene between the sensor head and the sample surface:

$$\frac{1}{\epsilon'_{r,adj}} = \frac{1}{\epsilon'_{r,p}} \left[\frac{t_p}{t_p + t_b} \right] + \frac{1}{\epsilon'_{r,b}} \left[\frac{t_b}{t_p + t_b} \right]\quad (6)$$

in which t represents the thickness of each layer and subscripts p and b represent the plastic and bulk layers, respectively.

How an electromagnetic wave will interact with an interface between regions of different dielectric properties is governed by the Fresnel equations – a broad set of principles describing the behaviour of light with different refractive indices n . By relating angles through Snell's law and assuming that the wave is entering the interface perpendicularly (i.e. $\theta_{incident} = \theta_{reflected} = \theta_{refracted} = 0$), $s-$ and $p-$ polarisations are equal, and the fraction of energy reflected can be represented by:

$$R = \left| \frac{n_2 - n_1}{n_2 + n_1} \right|^2\quad (7)$$

By recognising that $n = cv^{-1}$ (and therefore $n = \sqrt{\epsilon}$), this can be rewritten in terms of the relative permittivity, and used to model the reflection coefficient R . The transmission coefficient can similarly be determined from R , since $R + T = 1$. The scenario of an electromagnetic wave entering a building stone with $\epsilon_{b,r}$ from ambient air $\epsilon_{0,r}$ results in:

$$R = \left| \frac{\sqrt{\epsilon_{b,r}} - \sqrt{\epsilon_{0,r}}}{\sqrt{\epsilon_{b,r}} + \sqrt{\epsilon_{0,r}}} \right|^2\quad (8)$$

in which $\epsilon_{b,r}$ is the complex value, determined from the mixing model in Eq. (4). As geomaterials are generally lossy dielectrics with a loss tangent $\tan \delta > 0.1 = \epsilon''_r/\epsilon'_r$. When $\tan \delta > 0.1$ the contribution of the

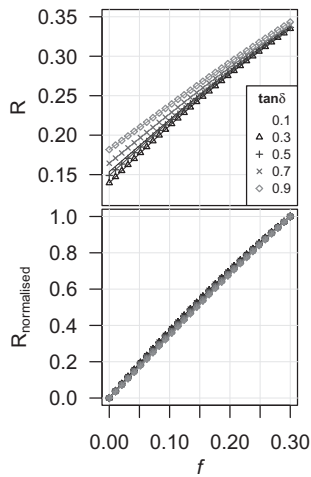


Fig. 3. Modelled reflection coefficients R for a lossy dielectric with $\epsilon'_r = 6.5$, with $0.1 < \tan\delta < 1$ for a range of water contents f . Coefficients are presented as original coefficients (upper plot) and as normalised values (lower plot), demonstrating that the 'characteristic curve' for R within this range is negligibly impacted by $\tan\delta$.

complex component of the effective permittivity to the reflection coefficient is much smaller than the contribution of changing water contents over realistic range of the latter in natural building stones. Although the complex component does influence R , especially at lower water contents (Fig. 3), it does not affect the shape of the curve. The reflection coefficient were used as a modelled reference as normalised values, emphasising the importance of the 'shape' of the relationship between water content. Due to uncertainties in the complex coefficient of the building stones studied herein, a value of $\tan\delta = 0.1$ was used for the reference models. It is important to note that this does not mean that a constant value was used for the component of relative permittivity (ϵ''_r), since $\epsilon''_r = \epsilon'_r \tan\delta$.

This can be used to model the reflection and transmission coefficients of an electromagnetic wave over a range of water contents. The coefficients for layered media can be represented by a matrix product of the layers or determined sequentially (Mazilu et al., 2001; Hehl and Wesch, 1980) or represented by a power series (Nečas and Ohlídal, 2014). A simulation was produced in R (version 3.3.3) for this purpose, based on the underlying mathematics in a defunct online tool (Gallant, 2018).

4. Results

Dielectric constants for dry samples (as determined with air- and metal-back measurements) are presented based on radar measurements (Section 4.1). These are used as the basis to model expected dielectric constants and reflection coefficients over a range of moisture contents for each stone type. These models are used as the comparative reference for evaluating calibrations of radar (Section 4.2) and microwave (Section 4.3) measurements, respectively.

4.1. Dry material dielectric constants

The dry dielectric constants ϵ'_b have been calculated with radar for three stone types (Table 2), by assuming $f = 0$ in Eq. (5) as described in Section 3. These represent the dielectric constant of the combined solid-air mixture of given minerals and porosity. Locharbriggs sandstone has the lower dielectric constant of the three stone types studied partially due to its greater porosity and lower bulk density; the two limestones, Portland and Clipsham, have similar porosities and as a result, similar dielectric constants. It is important to note that the values presented in Table 2 were calculated based on different samples of each

Table 2

Dielectric constants for three dry stone types ($n=1$) at 1.6 GHz calculated from radar travel times measured from two different calibration procedures.

| Stone | ϵ'_r | | | |
|--------------|----------------|--------------------|----------------|--------------------|
| | Air-back | | Metal-back | |
| | Ambient drying | Isolated diffusion | Ambient drying | Isolated diffusion |
| Portland | 3.87 | 3.81 | 3.74 | 3.67 |
| Clipsham | 3.81 | 3.99 | 3.74 | 3.99 |
| Locharbriggs | 1.47 | 1.86 | 1.43 | 1.81 |

stone type (see Table 1), and errors might be introduced by natural variation in physical properties (e.g. heterogeneity).

The calculated values of the dielectric constant are consistently lower for the metal-back measurements than those recorded with an air-back interface. Based on Eq. (1), this implies a higher signal travel time. Additionally, the variation in dielectric constants between samples and back interfaces are small ($\Delta < 0.14$) compared to the differences induced by changes in water content. It is possible that the position of peaks within the A-scans has been influenced by the ringing reflections caused by the presence of metal. The air-back values for the dielectric constant were therefore considered to be more reliable and were used to build modelled values of dielectric constant and reflection coefficients over a range of water contents.

4.2. Radar calibrations

Values of the dielectric constant and the direct wave amplitude of the high resolution radar are more closely related to modelled values for the isolated diffusion method than the ambient drying method. Fig. 4 demonstrates that values of the dielectric constant calculated from the ambient drying method are likely affected by an uneven distribution of moisture within the sample. This is represented by the parameters of linear regressions produced between the measured and modelled values of the dielectric constants (superimposed onto their respective subplots in Fig. 4). Values of R^2 represent the linearity of the relationship, while m represents the slope. An $m = 1$ represent a 1:1 relationship between the values, while $m < 1$ and $m > 1$ represent under-measured and over-measured values, respectively. The R^2 for models produced from the isolated diffusion calibrations are consistently higher than their ambient drying counterparts, and have values of m closer to 1. In general, the m values of the isolated diffusion procedure are < 1 , representing under-measurement.

At higher unsaturated water contents, values of ϵ'_r are lower than the modelled dielectric constants. This represents Stage I drying (Scherer, 1990; Cooling, 1930), in which the water content in the centre of the calibration sample has been reduced but the faces with evaporation remain pseudo-saturated with relatively constant flux. Since the radar measurements were taken at the centre of each face, the signal travel time is less than the gravimetric value would imply. At lower non-zero water contents, the calibration samples are in Stage II drying, in which there is a steeper moisture gradient (i.e. retention) at depth. The travel times at the centre of each face pass through the moisture remaining at depth in the calibration sample, which does not reflect the overall lower gravimetric value influenced by lower water contents near edges. As the models were based on dry dielectric constants determined from the samples, the modelled dielectric constant will always intersect with the measured value at $f = 0$.

The calculated dielectric constants for Locharbriggs are more closely related to models with $\alpha = 0.4$ in Eq. (5). It has been acknowledged that $\alpha > 0.5$ tends to result in an underestimation at higher water contents (Dobson et al., 1985; Knoll, 1996), a trend which is also observed for the calibration developed from ambient drying.

A similar comparison to dielectric constants can be drawn between measured direct wave amplitudes and transmission coefficients for

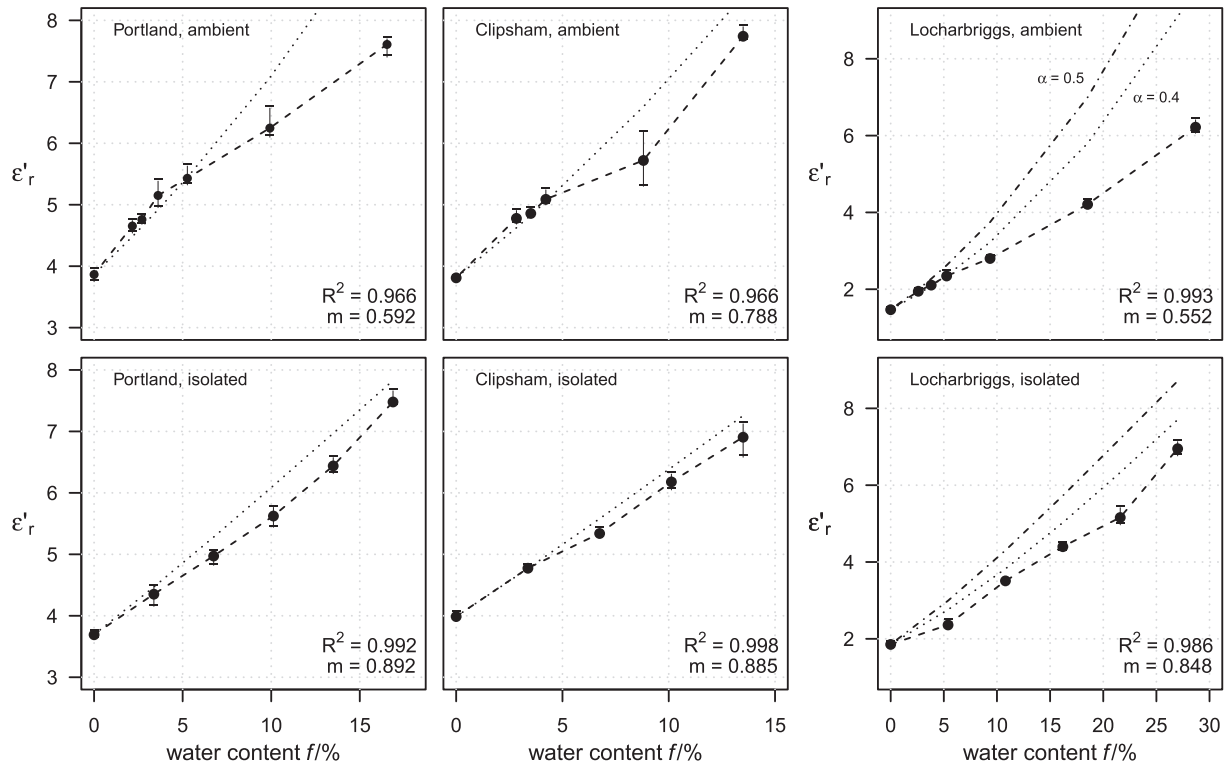


Fig. 4. Dielectric constants for three UK building stones at 1.6 GHz over the ambient saturation range of water contents, as calculated from radar measurements taken using two calibration procedures. Dotted lines are modelled dielectric permittivities based on the mixing model in Eq. (4). Vertical bars represent the range of measurements taken on each face of the sample. The same line types are used in both figures presenting results for Locharbriggs to represent values of α .

the two calibration methods (Fig. 5). The calibrations developed from isolated diffusion are consistent and more closely related to modelled transmission coefficients. As with the measured dielectric constants, the heterogeneous distribution of moisture within the samples causes an under-measurement at higher water contents and an over-measurement at lower water contents (compared to gravimetry). The underestimation at higher unsaturated water contents is less prevalent for the Portland calibration sample than that observed for the Clipsham and Locharbriggs samples. The deviations from the modelled transmission coefficients are more drastic for the direct wave amplitudes than the dielectric constants, except for the higher unsaturated water contents of the Portland calibration sample. Slopes of the linear regression results m are not presented in Fig. 5 as these are less meaningful for the scaled transmission coefficients.

This deviation from modelled behaviour is likely caused by the non-linear interactions between distributions of moisture and reflection/transmission of electromagnetic energy that can cause unintuitive ‘inversion’ of the coefficients. These principle can be demonstrated by simple cases of two-layer systems of porous media at different water contents. Fig. 6 shows the modelled reflection and transmission coefficients for a system with a total thickness of 150 mm and varying thickness of the upper layer. The solid line shows that, for a lower layer with a water content $f = 0$, the reflection coefficient can be reduced below the coefficient of a homogenous dry sample if there is a thin upper layer of water. Similarly, a lower layer with $f = 0.2$ covered by a thin dry upper layer can have a reflection coefficient amplified higher than a homogenous system with a higher water content. An amplifying inversion in the reflection coefficient is equivalent to a reducing inversion in the transmission coefficient, and vice versa. This inversion effect is likely exacerbating the aforementioned under- and over-estimations caused by an uneven distribution of water within the calibration samples. This is represented by more significant deviations observed in the direct wave amplitude compared with the modelled transmission coefficients.

4.2.1. Comparison of radar features for air-back and metal-back measurements

The radar features calculated over the range of water contents were very similar for a back interface of both metal and air. This was assessed with linear regression models between the dielectric constants and first wave amplitudes determined for the two calibration methods and type of back interface (Table 3). The models had regression coefficients $R^2 > 0.99$, except the dielectric constant determined by isolated diffusion for Locharbriggs ($R^2 = 0.906$) and the direct wave amplitude for Portland under isolated diffusion conditions ($R^2 = 0.855$). The regression model slopes were 1 ± 0.05 , representing a variability between measured parameters of less than 5%.

4.3. Microwave calibrations

The microwave sensor indices determined from isolated diffusion are generally more similar to the modelled reflection coefficients than those determined from the ambient calibration procedure for Portland and Clipsham samples. For the Locharbriggs, the correlation coefficients between the measured and modelled values are higher for the ambient drying procedure. Table 4 presents the linear regression parameters between the measured indices and the modelled reflection coefficients; slopes of the linear regression results m are not presented as these are less meaningful for the scaled reflection coefficients.

The combined effect of uneven distributions of water and inversion on sensor indices measured during ambient drying can be seen in Fig. 7. As the indices are proportional to the reflection coefficients, the over- and under-estimations are transposed from those seen in the direct wave amplitudes and transmission coefficients. The higher unsaturated water contents for some stone types and sensors are greater than a 1:1 proportionality with the modelled coefficients; at lower non-zero water contents, the indices are below proportionality to reflection coefficients.

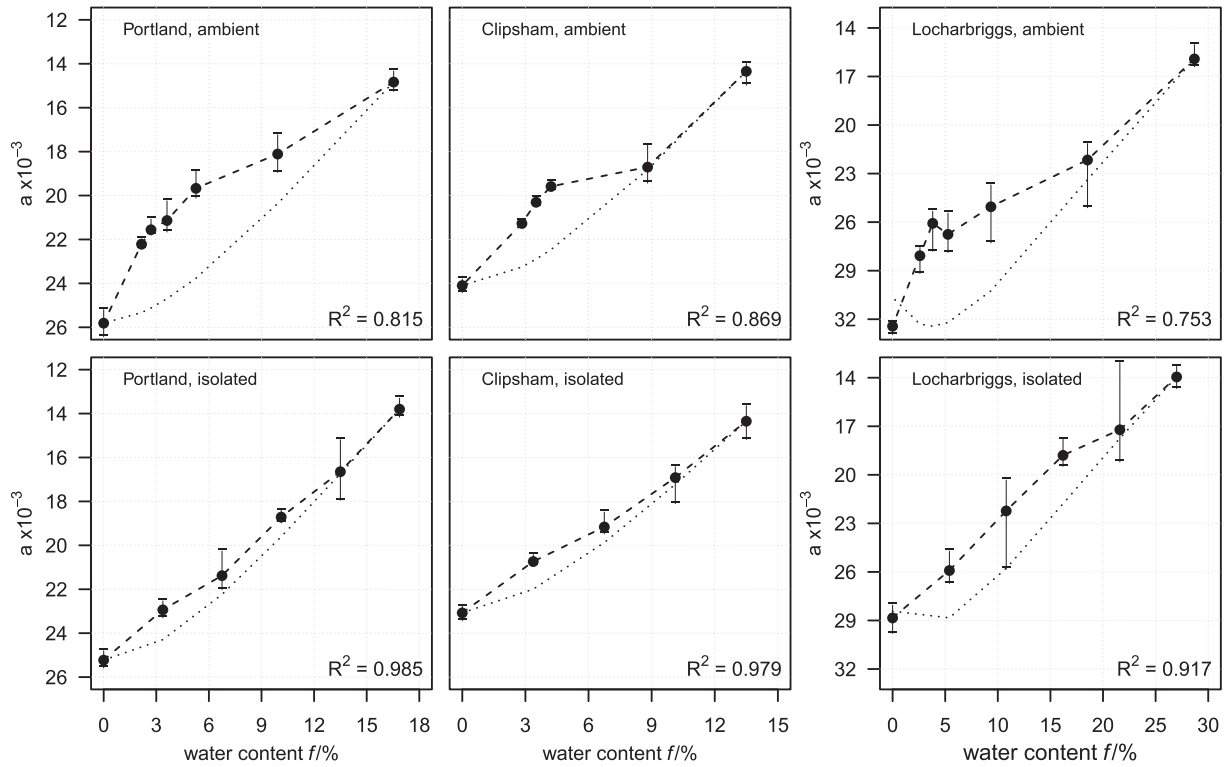


Fig. 5. Direct wave amplitude for three stone types at 1.6 GHz over the ambient saturation range of water contents, as calculated from radar measurements taken on two calibration procedures. Dotted lines are modelled transmission coefficients based on the mixing model in Eq. (4) assuming a loss tangent $\tan\delta = 0.1$, scaled between the extrema of the amplitudes. Vertical bars represent the range of measurements taken on each face of the sample.

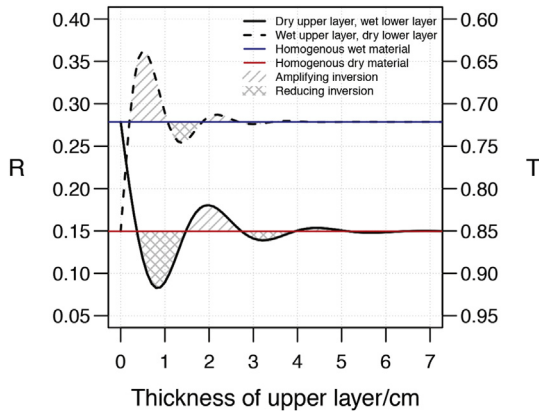


Fig. 6. Modelled reflection and transmission coefficients, R and T respectively, for two configurations of layered systems of a porous materials with $\epsilon_r = 6.3 - 0.63j$ (i.e. $\tan\delta = 0.1$). This demonstrates amplifying and reducing inversion of R for homogenous dry and wet ($f = 0.20$) geomaterials.

In some cases, proportionality to the modelled reflection coefficients dips below the homogenous dry calibration indices, e.g. Locharbriggs for the R and D sensor, and the two limestone types for the P sensor. There is also a corresponding strong amplifying inversion for the D sensor at non-zero lower water contents. As the depth penetration of the D sensor is between that of the R and P sensors, these corresponding inversions could be caused by higher moisture levels at mid-depths within the sample; unlike the examples presented in Fig. 6, these would be represented by a scenario in which there were three layers of alternating lower, higher, and lower water contents respectively.

5. Discussion

5.1. Calibration procedures

In contrast with existing literature (Bläuer and Rousset, 2009; Rousset and Bläuer, 2009; Møller and Olsen, 2011), both ambient drying and isolated diffusion calibration procedures yielded high quality calibration curves that related well to gravimetry over the full range of water contents. The isolated diffusion procedure yielded more

Table 3
Linear regression models for the calibrations developed from measurements taken with a metal back as a function of air-back measurements.

| | Ambient drying | | | Isolated diffusion | | |
|------------------------|----------------|----------|--------------|--------------------|----------|--------------|
| | Portland | Clipsham | Locharbriggs | Portland | Clipsham | Locharbriggs |
| Dielectric constants | | | | | | |
| R^2 | 0.999 | 0.997 | 0.999 | 0.997 | 1.00 | 0.906 |
| Intercept | -0.126 | 0.160 | 0.0360 | -0.0168 | 0.0848 | -0.463 |
| Slope | 1.01 | 0.961 | 0.997 | 1.00 | 0.978 | 1.05 |
| Direct wave amplitudes | | | | | | |
| R^2 | 0.994 | 0.997 | 0.992 | 0.855 | 1.00 | 1.00 |
| Intercept | -872 | -769 | 85.0 | -973 | 295 | 351 |
| Slope | 1.02 | 1.03 | 0.978 | 1.05 | 0.982 | 0.982 |

Table 4

Linear regression model R^2 values for the measured microwave sensor indices as a function of modelled reflection coefficients R normalised to the extrema of the index measured for each sensor and stone type.

| Microwave sensor | Portland | | Clipsham | | Locharbriggs | |
|------------------|----------|----------|----------|----------|--------------|----------|
| | Ambient | Isolated | Ambient | Isolated | Ambient | Isolated |
| R | 0.982 | 0.981 | 0.947 | 0.969 | 0.991 | 0.888 |
| D | 0.917 | 0.952 | 0.830 | 0.991 | 0.978 | 0.938 |
| P | 0.917 | 0.948 | 0.903 | 0.953 | 0.963 | 0.954 |

consistent calibration curves more closely related to modelled electromagnetic parameters.

Curves developed from the ambient drying procedure are impacted by a number of factors. Most importantly, the distribution of moisture during the drying process meant that radar and microwave measurements taken at the centre of each face were not indicative of the gravimetry. This was exacerbated by the non-linear interactions of the electromagnetic waves with the distributions of moisture that can cause inversions of the signal reflection and transmission. It is likely that these effects are especially strong for the sample size and

dimensions used, which was determined by the field of detection of the microwave measurement principle. The samples used herein have a volume-to-surface area ratio = 25. If samples have a smaller ratio, e.g. dimensions of 100 mm × 100 mm × 75 mm has a ratio = 15 (Eklund et al., 2013), the effects of moisture distribution and inversion are likely less pronounced for geophysical measurement techniques such as capacitance.

Ambient drying measurements taken at equal time intervals (24 h, in the procedure used herein) results in fewer measurements at higher water contents and a concentration of measurements at lower water contents. Increasing the measurement frequency for the beginning of the drying process is limited by the time required to collect the measurements: the time interval between measurements must be sufficiently longer than the time required to collect data with a set of measurement techniques so that the differences between gravimetric comparisons are valid for the measurement period.

The isolated diffusion procedure shows significant promise for producing calibrations relevant to cultural heritage and other non-destructive investigations of geomaterials. If measurements in the field are taken over a plastic grid as a spatial reference, the data would be more similar to calibration curves developed from the isolated

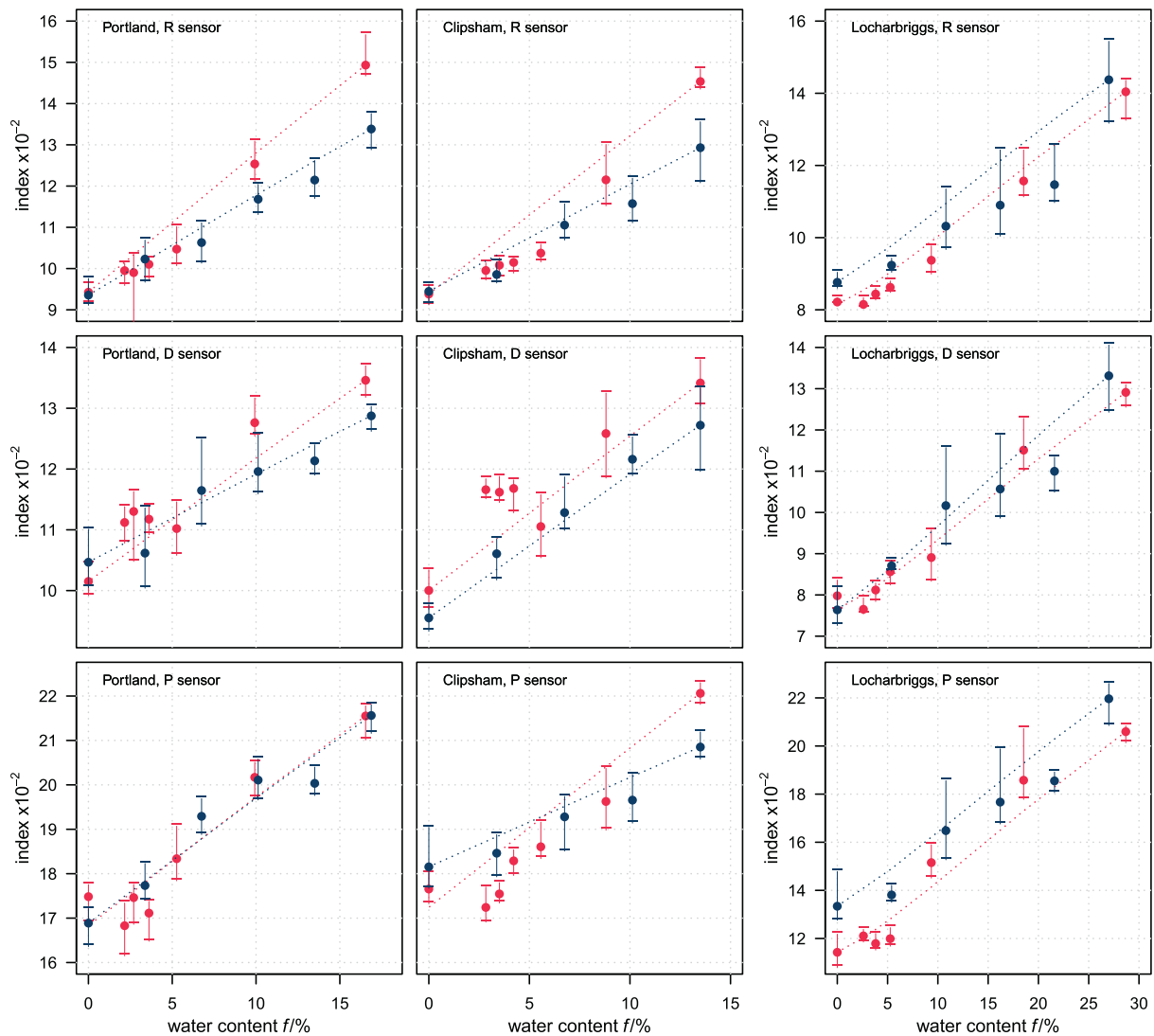


Fig. 7. Microwave sensor indices for three stone types over the ambient saturation range of water contents for ambient drying (red) and isolated diffusion (blue). Dotted lines are modelled reflection coefficients based on the mixing model in Eq. (4) assuming a loss tangent $\tan \delta = 0.1$, scaled between the extrema of the amplitudes. Vertical bars represent the range of measurements taken on each face of the sample.

diffusion procedure, which also introduces a plastic barrier between sensor and sample. The dielectric constant of many synthetic polymers is similar to that of polyethylene (Ahmad, 2012). If the calibrations and measurements were done with plastic grids of a different thickness, the parallel plate model (Eq. (6)) could be adapted to transform the measured readings into parameters equivalent with those of the calibration.

An important outcome of the calibrations developed for both radar features is that material heterogeneity between samples in the isolated diffusion method is negligible compared to the influence of changes in water content, which makes the isolated diffusion calibration technique viable. An important outcome of this result for heritage applications is that only one specimen is needed, which could support developing calibrations for scenarios in which sampling of materials is difficult. As the samples are in a state of near-equilibrium, the results of the isolated diffusion procedure are not impacted by time-dependent factors such as moisture loss—as is the case for ambient drying. It also facilitates inter-comparison of measurement techniques and the potential effect of environmental factors such as temperature and relative humidity. However, other calibration procedures, such as ambient drying, are still relevant and necessary for techniques that require direct contact with the sample surface, such as electrical resistance. Although it would be possible to remove the covering and re-seal the sample after the measurement, this would require more time and effort, and could affect the accuracy of future calibrations if moisture is evaporated during the process.

Radar parameters calculated from air-back and metal-back measurements are comparable. This is important for field measurements where a metal-back may be necessary to produce a sufficiently strong back-wall reflection that can be detected, especially important in constructions with walls or structural elements with thickness greater than the calibration samples used (150 mm).

5.2. Comparison of radar and microwave measurements

The radar output—measured dielectric constants and direct wave amplitude—was more consistently related to the gravimetric calibrations than the output from the microwave device. It is likely that the radar is more consistently calibrated and related to models due to more focused spatial measurement scale involved in its measurement principle. The spatial capture of a single radar measurement within an A-scan is based on the separation of the signal producing and receiving component which is quite small in a 1.6 GHz antenna. In contrast, the microwave sensors are field-based, with a non-discrete sensing volume—albeit decreasing with distance from the applicator. It is plausible that the microwave sensing technique is therefore more sensitive to external influences in the periphery of the measurement area.

Despite this, the microwave measurement system can be a useful tool in building surveying. It can be used to provide representations of moisture variation within a building fabric that are immediately interpretable on site. Measurements can be taken quickly over a flexible and large spatial scale as a range-finder method. Following this assessment, radar measurements could be taken for locations of specific interest. This is time-efficient, since the radar measurements typically involve the installation of a measurement grid or other system of alignment. The radar measurements requires further processing to produce numerical representations of the measured parameters, which means that results are not ready for interpretation while on site.

Importantly, the raw outputs from the two devices are not directly comparable. This demonstrates one utility of the calibration procedures: to use absolute water contents (as measured by gravimetry) as a common reference point to compare between the techniques. When comparing between radar and microwave measurements, it is important to remember proportionality. For example, the dielectric constants (derived from measured travel times) will be proportional to the microwave measurements. In contrast, any comparison or synthesis with

the direct wave amplitude should involve an inverse transformation of one of the parameters, since they are inversely proportional.

The calibrations developed demonstrate that the calculated and measured electromagnetic properties are not directly comparable between stone types. This is especially apparent as a contrast between the two limestones and the Locharbriggs sandstone. The permittivities of these materials are greatly dependent on their mineral composition and porosity, which also manifest as significant contrasts in the dielectric constant, direct wave amplitudes, and reflection/transmission coefficients. Natural building stones of similar mineralogies and porosities would therefore exhibit similar electromagnetic behaviour, i.e. parameters from non-destructive geophysical techniques would be similar. It is possible to predict what the dielectric constant—as the basis for most electromagnetic properties—will be, based on a given mineral composition and porosity (Martinez et al., 2001). This would enable an estimation of the ranges of non-destructive measurement techniques, based on prior knowledge of the range of other geomaterials.

6. Conclusion

Two calibration procedures based on ambient drying and isolated diffusion have produced calibration curves for radar and microwave techniques that relate well to gravimetry for three typical building stones in the UK. Both procedures produced comparable calibrations with air-back and metal-back interfaces. The isolated diffusion relates more closely to the modelled interactions of electromagnetic waves with porous media systems. The isolated diffusion procedure reduces the impact of uneven distribution of moisture within the samples and the potential for inversions of reflection and transmission. Thus, it is a viable low cost alternative that provides robust gravimetric calibration. This procedure also more closely reflects the qualities of in situ measurements if they are taken over a plastic grid for alignment, consistency, and surface protection.

Ambient drying remains a valid calibration technique that is less time and resource intensive than isolated diffusion. However, the calibration results for this procedure demonstrate the challenges of interpreting microwave moisture results when the distribution of moisture is uneven in a sample or in situ measurement. This procedure is especially relevant for measurement techniques that require direct surface contact or have smaller fields of detection. In the latter case, calibration curves can be developed on samples with smaller volume-to-surface area ratios which will be less impacted by uneven distributions of water within the samples.

These results demonstrate the utility of gravimetric calibrations for enabling comparability between measurement techniques and geomaterials. From these calibrations, mathematical relationships between sensor output and gravimetry can be developed. They enable a deeper understanding of the characteristic curves for different measurement devices and types of geomaterials, which supports accurate interpretation of survey information when it is not possible to develop material-specific calibrations.

Acknowledgements

We are grateful for the guidance on radar data handling provided by members of the 'Non-destructive Testing of Building Materials' division of the German Federal Institute for Materials Research and Testing (BAM), particularly the contributions of Sabine Kruschwitz and Jens Wöstmann. We also acknowledge the help of Sarah Hamilton and Callum Graham with data collection. We would like to thank an anonymous reviewer whose feedback which improved the employed method of data processing. Funding: This work was supported by the UK Engineering and Physical Sciences Research Council (EPSRC) grant for the Centre for Doctoral Training in Science and Engineering in Arts, Heritage

and Archaeology (EP/L016036/1). We acknowledge the support of Historic Environment Scotland and the Natural Sciences and Engineering Research Council of Canada (NSERC), funding reference number PGSD3-471105-2015.

References

- Ahmad, Z., 2012. Polymer dielectric materials. In: Silaghi, M.A. (Ed.), *Dielectric Material*. IntechOpen, Rijeka. Ch.1. <https://www.intechopen.com/books/dielectric-material/polymer-dielectric-materials>.
- ASTM International, 2013a. ASTM 7438-13 Standard Practice for Field Calibration and Application of Hand-Held Moisture Meters. ASTM, West Conshohocken, PA; USA.
- ASTM International, 2013b. ASTM D4444-13 Standard Test Method for Laboratory Standardization and Calibration of Hand-Held Moisture Meters. ASTM, West Conshohocken, PA; USA.
- ASTM International, 2016. ASTM D4442 16: Standard Test Methods for Direct Moisture Content Measurement of Wood and Wood-Based Materials. Standard, ASTM.
- ASTM International, 2011. D6432-11: Standard guide for using the surface ground penetrating radar method for subsurface investigation. R. ASTM Int.
- Binda, L., Cardani, G., Zanzi, L., 2010. Nondestructive testing evaluation of drying process in flooded full-scale masonry walls. *J. Perform. Constr. Facil.* 24 (5), 473–483.
- Birchak, J.R., Gardner, C.G., Hipp, J.E., Victor, J.M., 1974. High dielectric constant microwave probes for sensing soil moisture. *Proc. IEEE* 62 (1), 93–98.
- Birnbaum, G., Chatterjee, S., 1952. The dielectric constant of water vapor in the microwave region. *J. Appl. Phys.* 23 (2), 220–223.
- Bläuer, C., Rousset, B., 2009. Attempt to use microwave moisture mapping system (moist 200b) to control and monitor the water uptake of stones in frame of cultural heritage conservation. 12th International Conference on Microwave and High Frequency Heating (AMPERE 2009), pp. 29–32.
- Braun, R., Wilson, M., 1970. The removal of atmospheric sulphur by building stones. *Atmos. Environ.* 4 (4), 371–378.
- BSI, 2017. BS EN 16682, 2017. Conservation of cultural heritage. Methods of Measurement of Moisture Content, or Water Content, in Materials Constituting Immovable Cultural Heritage. Standard, British Standards Institution.
- Building Research Establishment, 2000. Technical Data Sheet: Locharbriggs Sandstone. <http://projects.bre.co.uk/ConDiv/stonelist/locharbriggs.html>.
- Camuffo, D., Bertolin, C., 2012. Towards standardisation of moisture content measurement in cultural heritage materials. *E-Preserv. Sci.* 9, 23–35.
- Cetrangolo, G., Domenech, L., Moltini, G., Morquío, A., 2017. Determination of moisture content in ceramic brick walls using ground penetration radar. *J. Nondestruct. Eval.* 36 (1), 12.
- Climent, M., Lindmark, S., Nilsson, L.-O., 2018. Calibration techniques. In: Nilsson, L.-O. (Ed.), *Methods of measuring Moisture in Building Materials and Structures: State-of-the-Art Report of the RILEM Technical Committee 248-MMB*. Springer International Publishing, pp. 27–37 Ch. 4.
- Cooling, L., 1930. Contribution to the study of florescence. II. The evaporation of water from bricks. *Trans. British Ceram. Soc.* 29, 39–54.
- Di Tullio, V., Proietti, N., Gobbino, M., Capitani, D., Olmi, R., Priori, S., Riminesi, C., Giani, E., 2010. Non-destructive mapping of dampness and salts in degraded wall paintings in hypogeous buildings: the case of St. Clement at mass fresco in St. Clement Basilica, Rome. *Anal. Bioanal. Chem.* 396 (5), 1885–1896.
- Dobson, M.C., Ulaby, F.T., Hallikainen, M.T., El-Raies, M.A., 1985. Microwave dielectric behavior of wet soil—part ii: Dielectric mixing models. *IEEE Trans. Geosci. Remote Sens.* 1, 35–46.
- Dubelaar, C., Engering, S., Van Hees, R., Koch, R., Lorenz, H., 2003. Lithofacies and petrophysical properties of Portland Base Bed and Portland Whit Bed limestone as related to durability. *Heron* 48 (3), 221–229.
- Eklund, J., Zhang, H., Viles, H., Curteis, T., 2013. Using handheld moisture meters on limestone: factors affecting performance and guidelines for best practice. *Int. J. Archit. Herit.* 7 (2), 207–224.
- Elkarmoty, M., Tinti, F., Kasmaeeyzadi, S., Bonduà, S., Bruno, R., 2018. 3d modeling of discontinuities using gpr in a commercial size ornamental limestone block. *Constr. Build. Mater.* 166, 81–86.
- Emery, D., Dickson, J., 1989. A syndepositional meteoric phreatic lens in the Middle Jurassic Lincolnshire Limestone, England, UK. *Sediment. Geol.* 65 (3–4), 273–284.
- Galagedara, L., Parkin, G., Redman, J., 2003. An analysis of the ground-penetrating radar direct ground wave method for soil water content measurement. *Hydrol. Process.* 17 (18), 3615–3628.
- Gallant, M., 2015. Layer Reflectance Calculator. Accessed via [www.archive.org http://www.jensign.com/reflect/r8TA.html](http://www.archive.org/http://www.jensign.com/reflect/r8TA.html) (Accessed on 11 April 2018).
- Gärtner, G., Plagge, R., Sonntag, H., 2010. Determination of moisture content of the outer wall using hf-sensor technology. Proceedings of the 1st European Conference on Moisture Measurement. Weimar October 5–7, 2010.
- Göller, A., 2001. Moisture mapping—getting 2D and 3D moisture distribution by microwave measurements. In: Kupfer, K. (Ed.), *Proc. 4th Intl. Conf. On Electromagn. Wave Interaction*. Weimar, pp. 282–289.
- Göller, A., 2006. Microwave scanning technology for material testing. Proceedings of the 9th European Conference on NDT. DGZfP- Proceedings BB September 25–29, 2006.
- Göller, A., 2012. Moist scan – multilayer microwave moisture scans at buildings, masonry and civil structures. Proceedings of the 14th International Conference and Exhibition on Structural Faults and Repair. Edinburgh July 3–5, 2012.
- Gummerson, R., Hall, C., Hoff, W., 1980. Capillary water transport in masonry structures: building construction applications of Darcy's law. *Construction papers*. vol. 1 pp. 17–27 1.
- Hall, C., Hoff, W., 2012. *Water Transport in Brick, Stone and Concrete*. 2nd ed. Spon Press, Taylor & Francis Group, London, New York.
- Hehl, K., Wesch, W., 1980. Calculation of optical reflection and transmission coefficients of a multi-layer system. *Phys. Status Solidi* 58 (1), 181–188 a.
- Inkpen, R., Viles, H., Moses, C., Baily, B., Collier, P., Trudgill, S., Cooke, R., 2012. Thirty years of erosion and declining atmospheric pollution at St Paul's Cathedral, London. *Atmos. Environ.* 62, 521–529.
- International Telecommunication Union, 2016. ITU Radio Regulations. International Telecommunication Union, Geneva.
- ISO, 2003. ISO 16979:2003 Wood-Based Panels – Determination of Moisture Content. Standard, International Standards Organisation.
- Jaynes, S.M., Cooke, R., 1987. Stone weathering in Southeast England. *Atmos. Environ.* 21 (7), 1601–1622.
- Klein, L., Swift, C., 1977. An improved model for the dielectric constant of sea water at microwave frequencies. *IEEE J. Ocean. Eng.* 2 (1), 104–111.
- Klysz, G., Balayssac, J.-P., 2007. Determination of volumetric water content of concrete using ground-penetrating radar. *Cem. Concr. Res.* 37 (8), 1164–1171.
- Knoll, M.D., 1996. A Petrophysical Basis for Ground Penetrating Radar and Very Early Time Electromagnetics: Electrical Properties of Sand-Clay Mixtures. Ph.D. thesis. University of British Columbia.
- Kurik, L., Kalamees, T., Kallavus, U., Sinivee, V., 2017. Influencing factors of moisture measurement when using microwave reflection method. *Energy Procedia* 132, 159–164.
- Lai, W.W.-L., Kind, T., Kruschwitz, S., Wöstmann, J., Wigggenhauser, H., 2014. Spectral absorption of spatial and temporal ground penetrating radar signals by water in construction materials. *NDT E Int.* 67, 55–63.
- Lai, W.W.-L., Dérobert, X., Annan, P., 2018 Jun 1. A review of ground penetrating radar application in civil engineering: a 30-year journey from locating and testing to imaging and diagnosis. *NDT & E Int.* 96, 58–78.
- Laurens, S., Balayssac, J., Rhazi, J., Klysz, G., Arliguie, G., 2005. Non-destructive evaluation of concrete moisture by gpr: experimental study and direct modeling. *Mater. Struct.* 38 (9), 827–832.
- Leary, E., 1983. *The Building Limestones of the British Isles*. Department of the Environment, Building Research Establishment.
- Leucci, G., Masini, N., Persico, R., 2012. Time–frequency analysis of gpr data to investigate the damage of monumental buildings. *J. Geophys. Eng.* 9 (4), S81.
- Lichtenecker, K., Rother, K., 1931. Die herleitung des logarithmischen mischungs-gesetzes aus allgemeinen prinzipien der stationären stormung. *Phys. Z.* 32, 255–260.
- Lundien, J.R., 1966. *Terrain Analysis by Electromagnetic Means: Report 2, Radar Responses to Laboratory Prepared Soil Samples*. Technical Report 3–693. Army Engineer Waterways Experiment Station, US.
- Mamillan, M., 1981. Alteration et durabilité des pierres. *Seminaire Alteration et Durabilité des Bétons et des Pierres*. St. Remy-Les-Chevreuse, France.
- Martinez, A., Byrnes, A.P., et al., 2001. Modeling dielectric-constant values of geologic materials: An aid to ground-penetrating radar data collection and Interpretation. *Kansas Geological Survey*. University of Kansas Lawrence, KS, USA.
- Martínez-Garrido, M., Fort, R., Gómez-Heras, M., Valles-Iriso, J., Varas-Muriel, M., 2018. A comprehensive study for moisture control in cultural heritage using non-destructive techniques. *J. Appl. Geophys.* 155, 36–52.
- Martinho, E., Dionísio, A., Almeida, F., Mendes, M., Grangeia, C., 2014. Integrated geophysical approach for stone decay diagnosis in cultural heritage. *Constr. Build. Mater.* 52, 345–352.
- Maxwell Garnett, J.C., 1904. Xii. Colours in metal glasses and in metallic films. *philosophical transactions of the royal society of London a: mathematical. Phys. Eng. Sci.* 203 (359–371), 385–420.
- Mazilu, M., Miller, A., Donchev, V.T., 2001. Modular method for calculation of transmission and reflection in multilayered structures. *Appl. Opt.* 40 (36), 6670–6676.
- Møller, E.B., Olsen, B., 2011. Rising damp, a reoccurring problem in basements—a case study with different attempts to stop the moisture. Proceedings in the 9th Nordic Symposium on Building Physics (NSB 2011).
- Nečas, D., Ohlídal, I., 2014. Consolidated series for efficient calculation of the reflection and transmission in rough multilayers. *Opt. Express* 22 (4), 4499–4515.
- Newton, R.W., 1977. Microwave remote sensing and its application to soil moisture detection. Technical Report RSC-81. A & M University, Texas.
- Olatinsu, O., Olorode, D., Oyedele, K., 2013. Radio frequency dielectric properties of limestone and sandstone from Ewekoro. *Eastern Dahomey Basin. Adv. Appl. Sci. Res.* 4, 150–158.
- Pandey, S.C., Pollard, A., Viles, H., Tellam, J., 2014. Influence of ion exchange processes on salt transport and distribution in historic sandstone buildings. *Appl. Geochem.* 48, 176–183.
- Pérez-Gracia, V., Capua, D.D., González-Drigo, R., Pujades, L., 2009. Laboratory characterization of a gpr antenna for high-resolution testing: Radiation pattern and vertical resolution. *NDT E Int.* 42 (4), 336–344.
- Pinchin, S.E., 2008. Techniques for monitoring moisture in walls. *Stud. Conserv.* 53 (S-2), 33–45.
- RILEM TC 177-MDT, 2005. 177-MDT 2005. MD. E. 1: Determination of moisture distribution and level using radar in masonry built with regular units. *Mater. Struct.* 38, 283–288.
- Rodríguez-Abad, I., Klysz, G., Martínez-Sala, R., Balayssac, J.P., Mené-Aparicio, J., 2016. Application of ground-penetrating radar technique to evaluate the waterfront location in hardened concrete. *Geosci. Instrum. Methods Data Syst.* 5 (2), 567–574.

- Rousset, B., Bläuer, C., 2009. R.0014.01f: Cathédrales de bâte, de berne, de fribourg et de lausanne: project de contrôle et de suivi des consolidants: résultats des teste de laboratoire. Tech. Rep. Conserv. Sci. Consult. Sàrl.
- Sahin, H., Ay, N., 2004. Dielectric properties of hardwood species at microwave frequencies. *J. Wood Sci.* 50 (4), 375–380.
- Saïd, M.N.A., 2007. Measurement methods of moisture in building envelopes—a literature review. *Int. J. Arch. Herit.* 1 (3), 293–310.
- Scherer, G.W., 1990. Theory of drying. *J. Am. Ceram. Soc.* 73 (1), 3–14.
- Senin, S., Hamid, R., 2016. Ground penetrating radar wave attenuation models for estimation of moisture and chloride content in concrete slab. *Constr. Build. Mater.* 106, 659–669.
- Sihvola, A., 2000. Mixing rules with complex dielectric coefficients. *Subsurf. Sens. Technol. Appl.* 1 (4), 393–415.
- Válek, J., Kruschwitz, S., Wöstmann, J., Kind, T., Valach, J., Köpp, C., Lesák, J., Oct. 2010. Non-destructive investigation of wet building material: multimethodical approach. *J. Perform. Constr. Facil.* 24 (5), 462–472.
- Yelf, R., 2004. Where is true time zero? Proceedings of the Tenth International Conference on Ground Penetrating Radar. Delft, pp. 279–282 21–24 June 2004
- Zhao, T., 2015. Effective Medium Modeling and Experimental Characterization of Multi-layer Dielectric with Periodic Inclusion. Ph.D. thesis. Iowa State University.